ARTICLE
Journal of Cellular Biochemistry 116:1232–1240 (2015)

Journal of Cellular Biochemistry

# Dynamic Mitochondrial Localisation of STAT3 in the Cellular Adipogenesis Model 3T3-L1

Adam H. Kramer,[1] Adrienne L. Edkins,[2] Heinrich C. Hoppe,[3] and Earl Prinsloo[1]*

[1]*Biomedical Biotechnology Research Unit, Biotechnology Innovation Centre, Rhodes University, PO Box 94, Grahamstown 6140, South Africa*

[2]*Department of Biochemistry and Microbiology, Biomedical Biotechnology Research Unit, Rhodes University, PO Box 94, Grahamstown 6140, South Africa*

[3]*Department of Biochemistry and Microbiology, Rhodes University, PO Box 94, Grahamstown 6140, South Africa*

## ABSTRACT

A mechanistic relationship exists between protein localisation, activity and cellular differentiation. Understanding the contribution of these molecular mechanisms is required for elucidation of conditions that drive development. Literature suggests non-canonical translocation of the Signal Transducer and Activator of Transcription 3 (STAT3) to the mitochondria contributes to the regulation of the electron transport chain, cellular respiration and reactive oxygen species production. Based on this we investigated the role of mitochondrial STAT3, specifically the serine 727 phosphorylated form, in cellular differentiation using the well-defined mouse adipogenic model 3T3-L1. Relative levels of reactive oxygen species (ROS) and the levels and dynamic localization of pSTAT3S727 were investigated during the initiation of adipogenesis. As a signalling entity, ROS is known to regulate the activation of C/EBPβ to stimulate a critical cascade of events prior to differentiation of 3T3-L1. Results indicate that upon induction of the differentiation programme, relative levels of mitochondrial pSTAT3S727 dramatically decrease in the mitochondria; in contrast the total cellular pSTAT3S727 levels increase. A positive correlation between increasing levels of ROS and dynamic changes in C/EBPβ indicate that mitochondrial STAT3 plays a potential critical role as an initiator of the process. Based on these findings we propose a model for mitochondrial STAT3 as a regulator of ROS in adipogenesis. J. Cell. Biochem. 116: 1232–1240, 2015. 

**KEY WORDS:** STAT3; MITOCHONDRIA; ADIPOGENESIS

The Signal Transducer and Activator of Transcription 3 (STAT3) mediates cellular differentiation, proliferation, survival and immune function within the cell [Levy and Lee, 2002]. Canonically, cytokine stimulated activation of cytoplasmic STAT3 drives membrane recruitment to specific receptors (e.g., gp130) resulting in phosphorylation at tyrosine-705 in the C-terminal Src-Homlogy 2 (SH2) domain by Janus Kinases (e.g., JAK2) and release and targeting to the nucleus, at equilibrium, for transcriptional activation [Ehret et al., 2001; Zhang and Darnell, 2001; Aaronson and Horvath, 2002]. Further to this it is established that STAT3 kinetically enters the nucleus unphosphorylated to bind to non-canonical DNA structures [Timofeeva et al., 2012].

Beyond the nucleus, STAT3 has been shown to localise to the mitochondria where it is thought to play a non-canonical role in regulation of oxidative phosphorylation [Wegrzyn et al., 2009; Reich, 2009]; this is still not fully understood, however it has been reported that it appears to maintain electron transport chain basal activity [Gough et al., 2009; Wegrzyn et al., 2009; Tammineni et al., 2013; Zhang et al., 2013].

Recently the importance of the phosphorylation of the serine 727 residue in the function of mitochondrial STAT3 has been noted. Zhang et al. [2013] have shown that mitochondrial STAT3 plays a potential crucial role in expansion of breast cancer. Through site directed mutagenesis experiments the group showed that the

Authors' contributions: AHK: Conception and design; acquisition of data; analysis and interpretation of data; preparation of manuscript. ALE: Analysis and interpretation of data; acquisition of flow cytometry data. HH: Analysis and interpretation of data. EP: Conception and design, analysis and interpretation of data; preparation of manuscript.

Grant sponsor: National Research Foundation; Grant sponsor: Department of Science and Technology; Grant sponsor: Kresge Foundation; Grant sponsor: Rhodes University.

*Correspondence to: Earl Prinsloo, Biomedical Biotechnology Research Unit, Biotechnology Innovation Centre, PO Box 94, Rhodes University, Grahamstown 6140, South Africa. E-mail: e.prinsloo@ru.ac.za

Manuscript Received: 30 September 2014; Manuscript Accepted: 19 December 2014

Accepted manuscript online in Wiley Online Library (wileyonlinelibrary.com): 6 January 2015

DOI 10.1002/jcb.25076 • © 2015 Wiley Periodicals, Inc.

phosphorylation at serine 727 had dramatic effects on tumour growth, the activity of complex I of the electron transport chain and the accumulation of reactive oxygen species (ROS) in the cell. Site directed mutagenesis experiments conducted by Tammineni et al. [2013] showed that a S727A mutation reduced the import of STAT3 and assembly into complex I by GRIM-19 (Genes associated with Retinoid-IFN-induced mortality-19); suggesting an additional role for this transactivation enhancing modification in mitochondrial localization.

A growing body of data regarding the non-canonical mitochondrial localisation of the STAT3 indicates a direct role for this signalling protein in the control of mitochondrial activity by interacting with complex I of the electron transport chain. Based on this we investigated the role for this localisation in cellular differentiation using the well-defined adipogenic mouse preadipocyte 3T3-L1 model [Green and Kehinde, 1974].

Reactive oxygen species (ROS) have been shown to play an important signalling role in adipocyte differentiation. CCAAT/Enhancer Binding Protein β (C/EBPβ) is a primary initiator of adipocyte differentiation and is typically expressed within two hours of stimulation with insulin, 3-Isobutyl 1-methylxanthine (IBMX) and dexamethasone. However, at this point C/EBPβ lacks DNA binding potential; possibly due to a lack of specific conformation dependent phosphorylation [Tang and Lane, 1999]. C/EBPβ only gains DNA binding potential 14 h after induction, and with DNA binding ability transcriptionally activates genes coding other important adipogenic transcription factors such as C/EBPα and Peroxisome Proliferator–Activated Receptor γ (PPARγ) through C/EBP regulatory elements [Tang et al., 2003]. In 3T3-L1 preadipocytes it has been shown that ROS facilitates differentiation by accelerating mitotic clonal expansion (MCE) [Lee et al., 2009]; increased levels of ROS result in C/EBPβ having greater DNA binding affinity which results in accelerated MCE and therefore greater differentiation efficiency. Furthermore, it was demonstrated that treatment of 3T3-L1 cells with $H_2O_2$ during differentiation resulted in accelerated cell cycle progression and that antioxidant treatment resulted in an arrest of MCE indicating that ROS must play a particularly important role during 3T3-L1 adipogenesis [Lee et al.,2009]. We therefore hypothesize that STAT3 may indirectly have a role in mediating ROS and adipogenesis in a non-canonical manner.

## MATERIALS AND METHODS

### 3T3-L1 ROUTINE CELL CULTURE AND DIFFERENTIATION

Murine preadipocyte 3T3-L1 cells (a kind gift from Prof. Carminita Frost, Nelson Mandela Metropolitan University) were routinely cultured and differentiated as previously described [Kramer et al., 2014]. Briefly, cells were maintained in Dulbecco's Modified Eagle's Medium supplemented with 5% (v/v) Foetal Calf Serum, 1% (w/v) L-Glutamine and 1% (w/v) penicillin/streptomycin/amphotericin B in a humidified 5% (v/v) $CO_2$ atmosphere at 37 °C. Cells were passaged at 80% confluence, as determined microscopically, through routine trypsinisation or differentiated two days post 100% confluence with media supplemented with 10 μg/mL insulin (NovoRapid), 0.25 μM dexamethasone (Sigma), 0.5 mM 3-Isobutyl 1-methylxanthine (IBMX) (Sigma) and 2 μM rosiglitazone (Sigma). Cells were maintained between days 3 and 4 in media supplemented with 10 μg/mL insulin. Cells were maintained in basal medium as described above 4 days post differentiation.

### ANALYSIS OF INTRACELLULAR LEVELS OF REACTIVE OXYGEN SPECIES (ROS)

Intracellular ROS levels were analysed based on a modified protocol described in Lee et al. [2009]. Briefly. trypsinised cells were resuspended to a density of $1 \times 10^6$ cells/mL in PBS (pH 7.4, 16 mM $Na_2HPO_4$, 2 mM $KH_2PO_4$, 137 mM NaCl, 3 mM KCl); 180 μL of the cell suspension was transferred to micro reaction tubes and 20 μL of 1 mM DCFH-DA (Sigma) was added to the cells (final concentration of 100 μM). The samples were incubated at 37 °C for 30 min. ROS levels were measured as fluorescence signal following excitation at 488 nm and emission detection at the 525/50 nm channel using flow cytometry (BD FACS Aria II SORP). Results were analysed using FlowJo v10.

### IMMUNOFLUORESCENCE STAINING

Primary antibodies used in the study included, rabbit C/EBPβ polyclonal IgG, rabbit anti-STAT3 (Ser 727) polyclonal IgG rabbit anti-pSTAT3 (Ser 727) polyclonal IgG, and goat anti-VDAC polyclonal IgG (Santa Cruz Biotechnology, Inc.). Cells were grown on borosilicate glass cover slips in six well culture plates (Nunclon™, Nunc). Medium was aspirated, and the cells were washed with PBS, before fixation for 30 min using a cold (4 °C) 4% (v/v) formaldehyde solution. Following fixation, cells were washed with PBS then permeabilized for 5 min with 0.1% Triton X-100 solution; followed by a set of three 5 min PBS washes. Coverslips were blocked for a minimum of 1 hour at room temperature using a 1% (w/v) BSA/PBS solution. Blocked cover slips were incubated with appropriate primary antibodies (1:500 dilution in 1% (w/v) BSA/PBS) overnight at 4 °C. The next morning the antibody solutions were aspirated and cover slips washed three times, 10 min per wash, with a 1% (w/v) BSA/PBS solution. Coverslips were then incubated with Alexa Fluor 488 chicken anti-rabbit IgG (H + L) or Alexa Fluor 546 donkey anti-goat IgG (H + L) (Life Technologies) (1:2000 dilution in 1% (w/v) BSA/PBS) in the dark at room temperature for a minimum of one hour before a final set of three 10 min washes with a 1% (w/v) BSA/PBS solution. Nuclear material was stained by dipping coverslips in a Hoechst 33342 (Sigma) solution (1μg/mL in water)) and cover slips were then allowed to dry before mounting with Dako fluorescent mounting medium (Dako). The same procedure was performed, without primary antibody, as a control. Samples were analysed using the Zeiss AxioVert.A1 Fluorescence LED Microscope and the Zeiss 510 Meta Confocal Laser Scanning Microscope. Images were captured in triplicate and analysed using the ImageJ ICA plugin [Li et al., 2004].

### ISOLATION OF MITOCHONDRIA

Fresh isolation buffer was prepared (0.3 M mannitol (Sigma), 0.1% BSA, 0.2 mM EDTA, 10 mM HEPES) and the pH adjusted to 7.4 using KOH. The buffer was chilled on ice and protease inhibitor cocktail

(Sigma) added prior to use (1:100 dilution). Cells were trypsinized and washed with cold PBS. Cells were counted via trypan blue staining. Following the PBS wash, between $30 \times 10^6$ and $50 \times 10^{-6}$ cells were pelleted via centrifugation at 800 *g* for 2 min per isolation. The resulting pellets were resuspended in cold isolation buffer (five times the pellet volume) and transferred to a 1 mL micro reaction tube. The cell suspension was then homogenized on ice using a plastic Dounce homogenizer. When over 70% of cells had been ruptured, as determined by trypan blue staining, the homogenate was subjected to centrifugation at 1000 *g* for 10 min to remove whole cells and nuclei. The supernatant was collected and subjected to further centrifugation at 15,000 *g* for 15 min. The supernatant, representing the cytosolic fraction was removed and stored, and the pellet, representing the mitochondrial fraction washed twice in cold isolation buffer prior to being processed for SDS-PAGE [Laemmli, 1970] and western blot analysis.

### WESTERN BLOT ANALYSIS

Antibodies used in the western blot analysis were as previously described above with the addition of rabbit anti-Prohibitin polyclonal IgG (Santa Cruz Biotechnology, Inc.) and rabbit anti-Histone H3 polyclonal IgG (Cell Signalling Technologies). Cells were collected via trypsinization and viable cells enumerated by 0.4% (w/v) trypan blue staining. Cells were lysed in Laemmli sample buffer supplemented with 5% (v/v) β-mercaptethanol (BioRad) at 95 °C for 10 min. Following SDS-PAGE electrophoresis [Laemmli, 1970] and transfer onto 0.22 μm PVDF filter membranes (BioRad), membranes were blocked for 1 h at room temperature with 5% (w/v) skim milk in a TBS-Tween 20 buffer. Blocking was followed by an overnight incubation at 4 °C with the relevant primary. The membrane was then washed and incubated with horseradish peroxidise conjugated goat anti-rabbit IgG (Santa Cruz Biotechnology, Inc.) for 1 h at room temperature. After washing, the membrane was developed with Clarity Western ECL Substrate (BioRad) according to the manufacturer's instructions. Images were captured using the UVTec Prochemilumence System.

## RESULTS AND DISCUSSION

Previous descriptions of increased intracellular ROS during early adipogenesis were associated with the facilitation of MCE [Lee et al., 2009], here, we performed a dichloro-dihydro-fluorescein diactetate (DCFH-DA) flow cytometric assay to validate previous reports; upon oxidation DCFH-DA is de-esterified to the fluorophore. 2′,7′-dichlorofluorescein. Intracellular levels of ROS within 3T3-L1 cells steadily increased upon the induction of differentiation for 4 days as shown by Zebra plots, after which levels were found to reduce (Fig. 1A).

The results presented here show that 3T3-L1 cells have increased levels of ROS for the first four days of differentiation. This result correlates with the increased expression levels (in relation to the Histone H3 loading control; total cellular protein from cell lysates shown) and nuclear localisation of C/EBPβ during adipogenesis as shown in Figure 1B and C. It is important to note that C/EBPβ has two major isoforms (38 and 18 kDa). It has been shown that isoform expression is differentially regulated at the translational level [Tang and Lane, 1999; Kim et al., 2008]. While, total cellular levels of C/EBPβ, shown here by western blot, remain constant relative to the loading control (Fig. 1C), time dependent distinct changes in gross localisation is observed (Fig. 1C) which correlates with increased intracellular ROS.

The localisation of the serine 727 phosphorylated STAT3 (pSTAT3S727) was investigated. As comparison, the localisation of total cellular STAT3 is shown over the same time period (Fig. S1). Preadipocytes were found to have nuclear localised pSTAT3S727 (80% of cells observed, n = 24). Staining for pSTATS727 in preadipocytes revealed slight punctate and reticulate staining. Upon differentiation, Figure 2A, Day 1, nuclear staining persisted (87%, n = 53) while there was a definite increase of pSTAT3S727 signal detected in the cytoplasm of cells as shown in Figure 2A, Day 1.

On Day 2, nuclear staining became less distinct while cytoplasmic staining became more prominent with only 51% of observed cells (n = 64) having nuclear staining, and by Day 3 nuclear staining was not observed at all (n = 50). Cytoplasmic staining on Day 3 revealed distinct punctate structures as highlighted by red arrows in Figure 2A, Day 3. This staining pattern persisted to Day 4 (74%, n = 43). Supplementary Fig S2 shows the nuclear localisation of pSTATS727 starting to return 5 days post-induction (42%, n = 70) and becoming more distinct on Day 6 (53%, n = 34) (Fig. S2, Day 6); the decreased nuclear localisation of total STAT3 is observable in Figure S1, Day 3, although it should be noted that total STAT3 staining in Figure S1, Day 4 shows a nuclear accumulation 48 h prior to the increased nuclear accumulation of pSTAT3S727 indicating time dependent defined compartmentalised populations of STAT3.

The total cellular levels of pSTAT3S727 were investigated through Western blotting and densitometric analysis. Results indicated that levels of pSTAT3S727 followed an increasing trend during differentiation as shown in Figure 2B and C with levels at Day 6 found to be the relative highest. One distinct band at approximately 90 kDa was routinely detected when probing for pSTAT3S727 indicating that pSTAT3S727 is potentially the larger α isoform as would be expected [Ng et al., 2012]. Based on this the subcellular distribution, specifically the mitochondrial localisation of pSTAT3S727, was investigated to test whether a similar trend was observable.

Co-localisation analysis between the mitochondrial marker, Voltage Dependant Anion Channel (VDAC) and pSTAT3S727, the proposed mitochondrial-localised isoform of STAT3 was performed on induced and differentiating 3T3-L1 preadipocytes to determine whether there was a change in the mitochondrial localisation of pSTAT3S727 during adipogenic events.

Product of the Differences of the Mean (PDM) images highlight regions of co-localisation based on the PDM for each pixel and were generated by the Intensity Correlation Analysis plugin available in ImageJ [Li et al., 2004]. Positive PDM values are correlated with co-localisation. As seen in Figure 3, two PDM images are generated. The first shows both positive PDM values in yellow and negative values in blue, and the second highlights only pixels with positive values.

As seen in Figure 3, in the imaged Day 0 sample pSTAT3S727 was found predominantly in the nucleus with some punctate cytoplasmic staining observed (consistent with the epifluorescence staining patterns in Fig. 2A, Day 1) while VDAC was distinctly cytoplasmic.

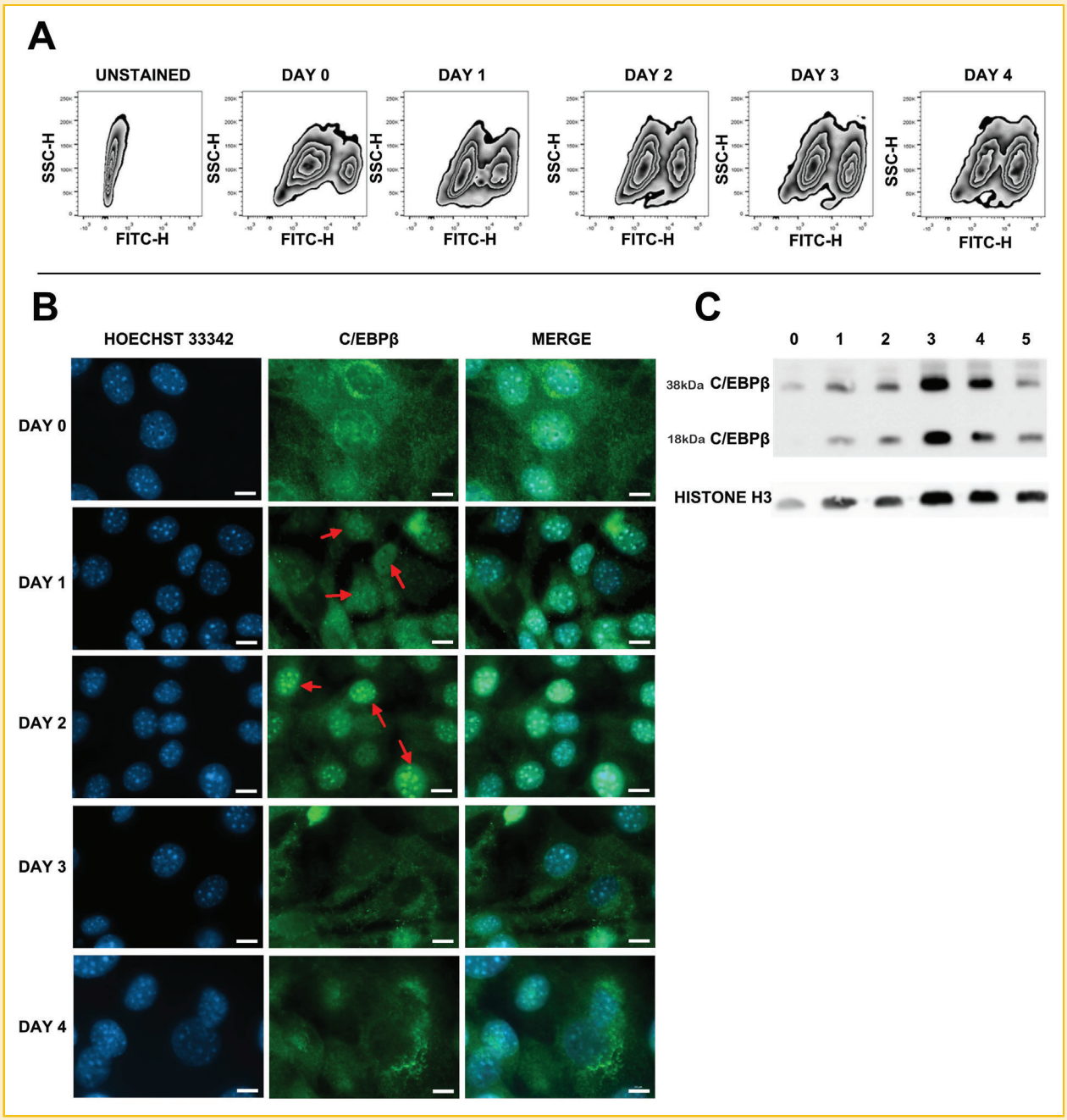


**Fig. 1.** Reactive oxygen species levels, expression and localisation of C/EBPβ during adipocyte differentiation. (A) Zebra plot of FITC-H (DCF-DA fluorescence) against SSC (granularity) of differentiating 3T3-L1 preadipocytes stained with DCF-DA through days 0–4 of differentiation. Samples were either unstained or incubated in the presence of DCF-DA . Defined regions indicate increased differentiation (Higher ROS levels and increased granularity) (B) Immunofluorescence analysis of the localisation of C/EBPβ through days 0–4 of differentiation. Red arrows highlight nuclear localised C/EBPβ during days 1 and 2 post-induction. Scale bars = 10 μm. (C) Western blot analysis of pre- (Day 0) and post- (Days 1–5) induction of adipocyte differentiation. Histone H3 was used as a loading control. Equal loading was achieved through viable cell enumeration and 225 000 cell/lane was loaded on SDS-PAGE.

The generated PDM image revealed punctate structures in some cells and the resulting scattergram indicates a level of overlap. In the Day 1 panel nuclear localised pSTAT3S727 is no longer observed, while VDAC staining remains non-nuclear; in fact distinct perinuclear punctuate staining patterns are observable for both pSTAT3S727 and VDAC channels. The resulting scattergram reveals slightly increased independent pSTAT3S727 staining (red channel). There are distinct co-localised punctate areas in observed cells indicated by the PDM image. The Day 2 panel reveals cytoplasmic staining for both proteins with PDM images revealing very little co-localisation in any cells in the image and a decrease in the perinuclear assemblies observed in Day 1. The resulting scattergram

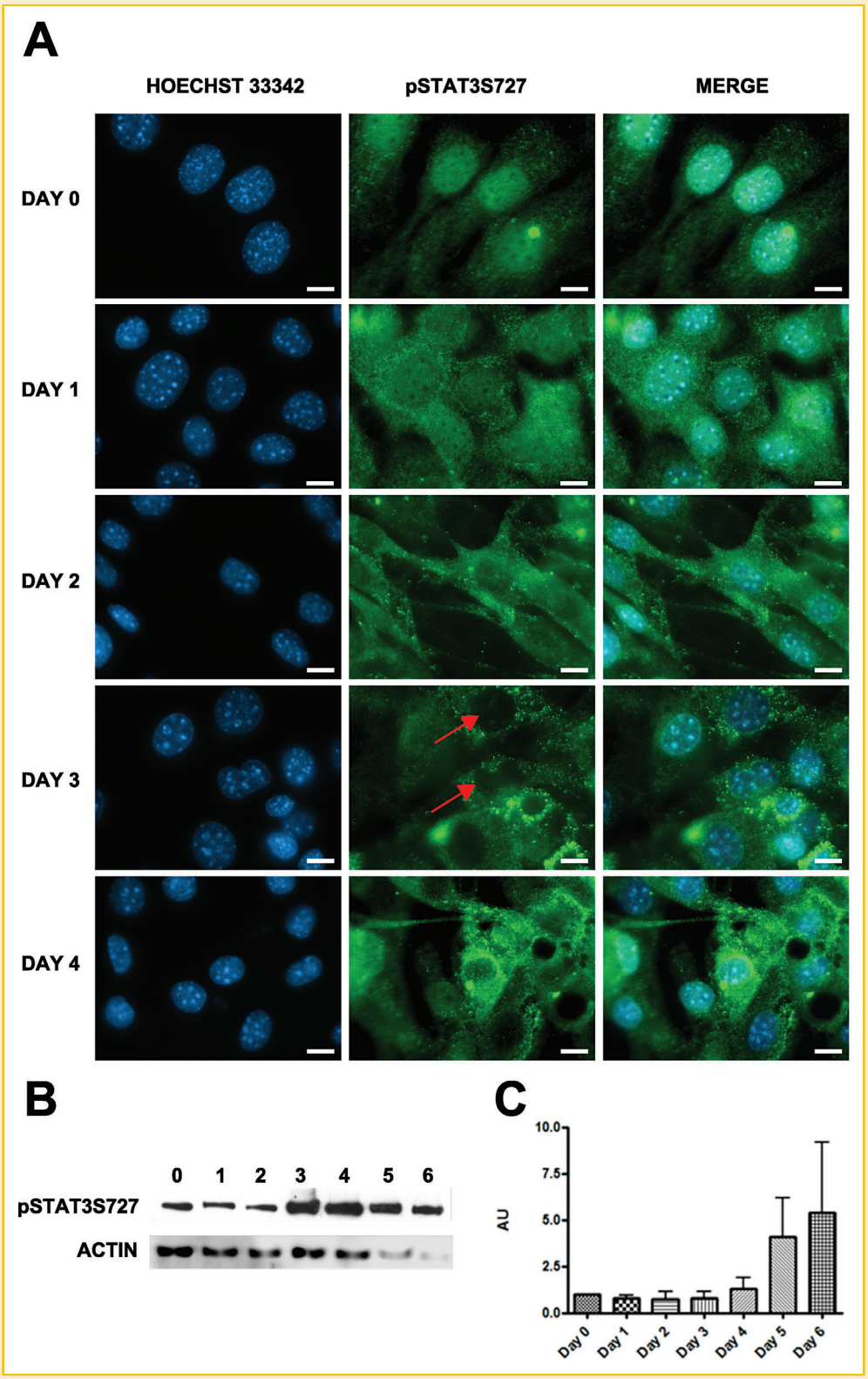


**Fig. 2.** Localisation and levels of pSTAT3S727 during 3T3-L1 adipocyte differentiation. (A) Immunofluorescence analysis of the localisation pSTAT3S727 through days 1–6 of 3T3-L1 adipocyte differentiation. Red arrows highlight the loss of nuclear localisation on Day 3. Scale bars = 10 μm. Images were captured using a Zeiss AxioVert.A1 FL-LED Fluorescence Microscope. Analysis was performed at 1000× magnification. Images representable of multiple images (n = 6). (B) Western blot of pSTAT3S727 through days 0–6 of differentiation. Cell were enumerated and used for equal loading (225,000 cells/per lane), pSTAT3S727 detected signal was normalised against actin as a loading control (n = 3). (C) Densitometric analysis of levels of pSTAT3S727, normalised to actin, during differentiation (n = 3). Data was plotted using GraphPad Prism V4.0.

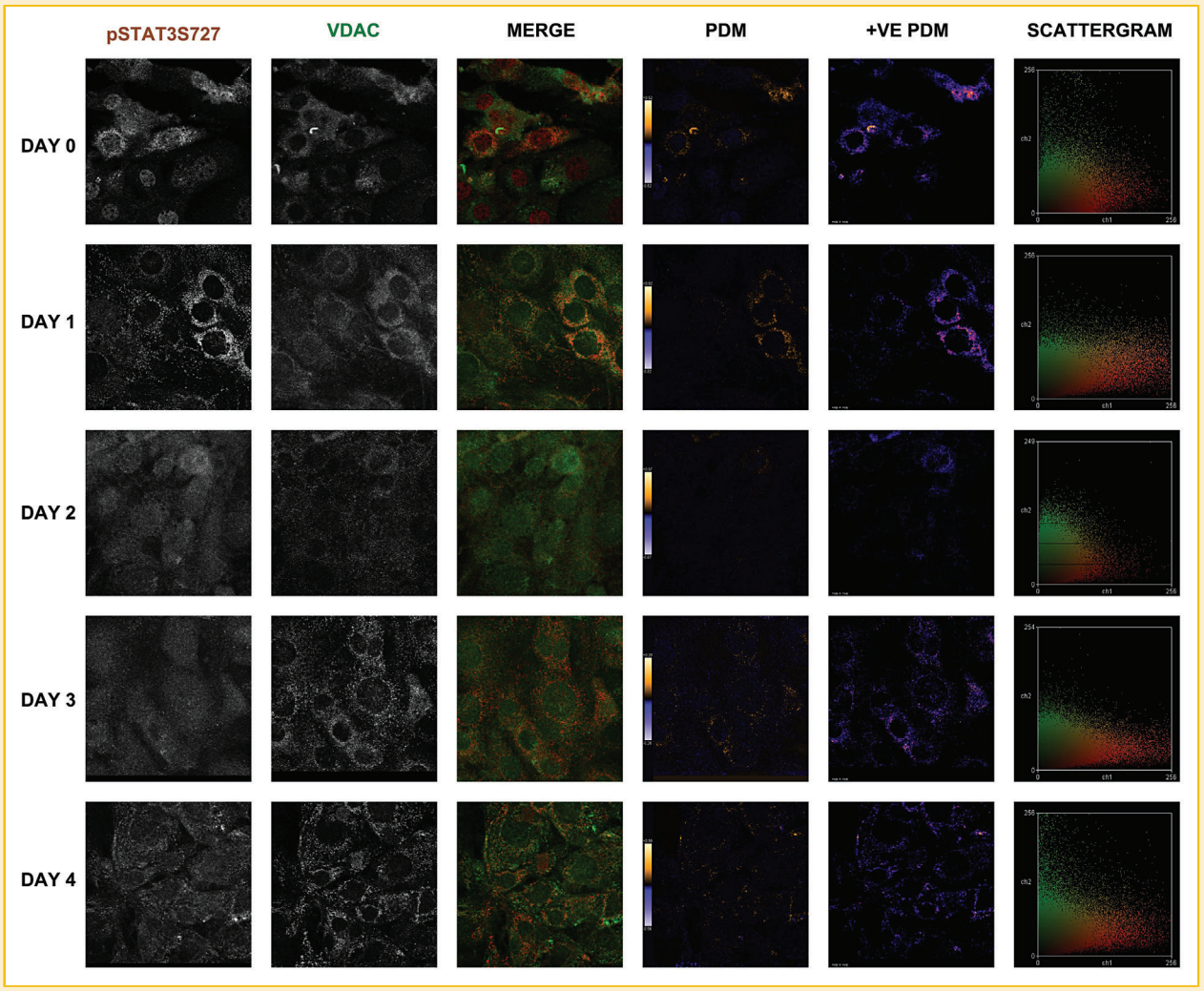


**Fig. 3.** Co-localisation analysis of pSTAT3S727 and VDAC in differentiating 3T3-L1 preadipocytes. Preadipocytes were induced to differentiate and subjected to immunofluorescence staining as previously described. Images were captured using the Zeiss LSM 510 Meta confocal microscope and co-localisation analysis was performed using ImageJ software (NCBI). Panels represent: the red channel (pSTAT3S727), green channel (VDAC); PDM images highlighting co-localised pixels in yellow and segregated pixels in blue; positive PDM pixels only.

indicates little overlap between the two channels. Next, the Day 3 image showing cytoplasmic staining of both VDAC and pSTAT3S727, and the PDM images shows that some cells have punctate co-localised areas in the cytoplasm and the resulting scattergram shows a level of overlap with more independent pSTAT3S727 staining again observed. Similar observations were made on Day 4, with a few cells having positive PDM values. The perinuclear staining patterns for VDAC was observed to return on Day 3 and 4 with some co-localisation with pSTAT3S727 on Days 3 and 4. Interestingly, the increased perinuclear staining of VDAC observed correlates with the increased intracellular ROS (Fig. 1A). This is similar to the ROS-dependent mitochondrial clustering reported by Al-Mehdi et al. [2012] in rat pulmonary artery endothelial cells and the perinuclear clustering and altered mitochondrial dynamics observed by Kita et al. [2009] in 3T3-L1 cells where triacylglycerol accumulation was reported as partly regulated by global mitochondrial fission and fusion events.

PDM based co-localisation analysis was performed by counting cells displaying distinctly positive PDM values and displaying typical mitochondrial like structures as seen in PDM generated images in Figure 3. Multiple slides and randomised (to the Hoechst 33342 nuclear staining) multiple fields of view were used in the analysis. During 3T3-L1 differentiation, analysis revealed that more cells had positive PDM values during Days 0 (55%, $n = 42$) and 1 (48%, $n = 33$) of differentiation. Incidences of cells with positive PDM values decreased during Days 2 (33%, $n = 60$) and 3 (45%, $n = 54$).

Mitochondria were next isolated from differentiating 3T3-L1 preadipocytes cells and probed for pSTAT3S727 to determine firstly, whether pSTAT3727 would be detected and, secondly if detected, whether the levels of pSTAT3S727 changed within mitochondria during differentiation as shown by confocal laser scanning microscopy (Fig. 3). Isolated mitochondrial samples were probed for Actin and Lysosomal-associated membrane protein 1 (LAMP1) to

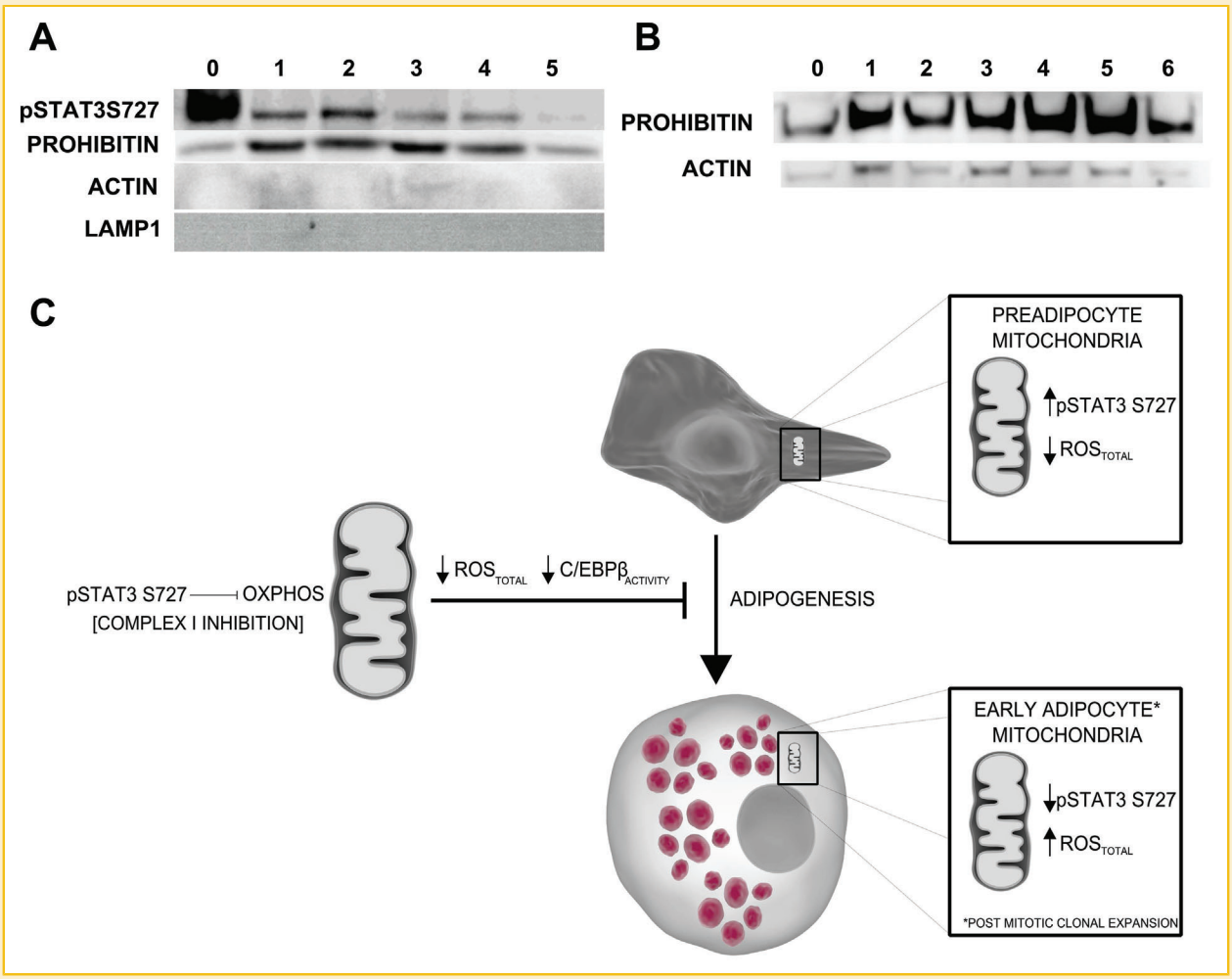


**Fig. 4.** Mitochondrial pSTAT3S727 levels decrease during early adipogenesis. (A) Levels of pSTAT3S727 within isolated mitochondria during 3T3-L1 differentiation. Mitochondria were isolated from differentiating cells on day 0–5 and subjected to Western blot analysis (20 μg per lane) to determine levels of pSTATS727. The mitochondrial marker Prohibitin was used as a loading control. Blots were probed for Actin and LAMP1 to determine levels of cytoplasmic and lysosomal/endosomal contamination, respectively. (B) Total cellular Prohibitin levels relative to total cellular actin over a 6 day time course. (C) Proposed hypothesis model for the potential role of observed mitochondrial localisation changes of pSTAT3 S727 on the early differentiation of mouse preadipocytes. See text for further details.

determine levels of cytoplasmic and endosome [Xu et al., 2007] contamination, respectively. Actin and LAMP1 were not detected in any samples as shown in Figure 4A. Prohibitin was used as a mitochondrial marker. Figure 4B shows prohibitin levels increasing in total cell extracts relative to actin levels indicating potential mitochondrial biogenesis.

Serine 727 phosphorylated STAT3 was detected in all mitochondrial samples and observation revealed that levels were highest in mitochondria isolated from uninduced undifferentiated cells as shown in Figure 4A (Day 0) and decreased to basal levels through mitotic clonal expansion and the initial phase of adipogenesis (Day 1–5).

## CONCLUSION

Based on this data it is hypothesized that STAT3 is potentially involved in modulating levels of ROS during differentiation. STAT3 has been implicated in activating the Warburg effect [Demaria et al., 2010] in a canonical manner by regulating the expression of certain genes such as HIF-1α and therefore affecting ROS levels. However, STAT3 may be regulating ROS in a more direct non-canonical manner. It is known that STAT3 interacts directly with GRIM-19, a subunit of complex I of the mitochondrial electron transport chain [Tammineni et al., 2013]. Complex I activity is directly linked to ROS production [Hirst et al., 2008]. Interestingly it has been shown that the nuclear localisation sequence, DNA-binding domain, the SH2 domain and tyrosine 705 of the STAT3 molecule are not required for the actions of mitochondrial pSTAT3S727 [Zhang et al., 2013]. This suggests that mitochondrial STAT3 must be the longer α isoform as was confirmed in the current study presented here.

Data presented here show that levels of mitochondrial STAT3 change during the differentiation process, suggesting that STAT3 is playing a role in mitochondrial respiration and ROS production. This

is in contrast to the observable increase in total pSTAT3S727 during a 6 day time course of initial adipogenesis. The question remains, if STAT3 is actively regulating ROS production in the mitochondria, how does this process work? Zhang et al. [2013] showed that phosphorylation of serine 727 of STAT3 enhanced coupling of complex I and resulted in decreased production of ROS in 4T1 mouse mammary carcinoma cells. This result may explain why lower levels of mitochondrial pSTAT3S727 were found in differentiating cells. When cells are induced to differentiate, levels of ROS increase. If STAT3 functions in the mitochondria to reduce ROS levels, upon induction mitochondrial STAT3 levels may decrease allowing for higher levels of ROS to be produced.

Higher levels of ROS have been shown to play an important role during adipogenic differentiation. It has been reported that ROS production at complex III regulates adipogenesis of human mesenchymal stem cells [Tormos et al., 2011]. Further to this, it has been shown that higher levels of ROS within differentiating 3T3-L1 cells accelerate mitotic clonal expansion and increase the differentiation efficiency [Lee et al., 2009]. The primary action of ROS within differentiating 3T3-L1 cells may be on the DNA binding efficiency of CCAAT/enhancer binding protein β. As discussed previously, C/EBPβ is an early adipogenic protein expressed within the first few hours of adipocyte differentiation. Interestingly, C/EBPβ DNA binding has been shown to be enhanced by oxidation and that increased levels of ROS result in enhanced C/EBPβ DNA binding activity [Lee et al., 2009]. It was found that levels of ROS correlated with the nuclear localisation of C/EBPβ in this study. It was too shown that levels of mitochondrial STAT3 were reduced upon induction of differentiation. We therefore propose the model presented in Figure 4C to explain the potential role of mitochondrial STAT3 in the regulation of ROS during the initiation of adipogenesis. This reduction of mitochondrial STAT3 may be the cause of increased levels of ROS as a result of increased oxidative phosphorylation (OXPHOS) due to STAT3′s inhibitory effect on complex I, which in turn results in enhanced DNA binding of adipogenic transcription factors such as C/EBPβ, allowing for efficient adipocyte differentiation.

## ACKNOWLEDGEMENTS

The authors acknowledge the National Research Foundation (NRF), Department of Science and Technology (DST), the Kresge Foundation and Rhodes University for funding, www.somersault1824.com for their Library of Science Illustrations and Prof. Carminita L Frost (NMMU) for the 3T3-L1 cells and manuscript critique. AHK is a recipient of a NRF Scarce Skills Scholarship.

## REFERENCES

Aaronson DS, Horvath CM. 2002. A road map for those who don't know JAK-STAT. Science 296:1653–1655.

Al-Mehdi A, Pastukh VM, Swiger BM, Reed DJ, Patel MR, Bardwell GC, Pastukh VV, Alexeyev MF, Gillespie MN. 2012. Perinuclear mitochondrial clustering creates an oxidant-rich nuclear domain required for hypoxia-induced transcription. Sci Signal 5:ra47.

Demaria M, Giorgi C, Lebiedzinska M, Esposito G, D′Angeli L, Bartoli A, Gough DJ, Turkson J, Levy DE, Watson CJ, Wieckowski MR, Provero P, Pinton P, Poli V. 2010. A STAT3-mediated metabolic switch is involved in tumour transformation and STAT3 addiction. Aging (Albany NY) 2:823–842.

Ehret GB, Reichenbach P, Schindler U, Horvath CM, Fritz S, Nabholz M, Bucher P. 2001. DNA binding specificity of different STAT proteins. Comparison of in vitro specificity with natural target sites. J Biol Chem 276:6675–6688.

Gough DJ, Corlett A, Schlessinger K, Wegrzyn J, Larner AC, Levy DE. 2009. Mitochondrial STAT3 supports Ras-dependent oncogenic transformation. Science 324:1713–1716.

Green H, Kehinde O. 1974. Sublines of mouse 3T3 cells that accumulate lipid. Cell 1:113–116.

Hirst J, King MS, Pryde KR. 2008. The production of reactive oxygen species by complex I. Biochem Soc Trans 36:976–980.

Kim MH, Fields J, Field J. 2008. Translationally regulated C/EBP beta isoform expression upregulates metastatic genes in hormone-independent prostate cancer cells. Prostate 68:1362–1371.

Kita T, Nishida H, Shibata H, Niimi S, Higuti T, Arakaki N. 2009. Possible role of mitochondrial remodelling on cellular triacylglycerol accumulation. J Biochem 146:787–796.

Kramer AH, Joos-Vandewalle J, Edkins AL, Frost CL, Prinsloo E. 2014. Real-time monitoring of 3T3-L1 preadipocyte differentiation using a commercially available electric cell-substrate impedance sensor system. Biochem Biophys Res Commun 443:1245–1250.

Laemmli UK. 1970. Cleavage of structural proteins during the assembly of the head of bacteriophage T4. Nature 227:680–685.

Lee H, Lee YJ, Choi H, Ko EH, Kim J-w. 2009. Reactive oxygen species facilitate adipocyte differentiation by accelerating mitotic clonal expansion. J Biol Chem 284:10601–10609.

Levy DE, Lee CK. 2002. What does Stat3 do? J Clin Invest 109:1143–1148.

Li Q, Lau A, Morris TJ, Guo L, Fordyce CB, Stanley EF. 2004. A syntaxin 1, Galpha(o), and N-type calcium channel complex at a presynaptic nerve terminal: Analysis by quantitative immunocolocalization. J Neurosci 24:4070–4081.

Ng IHW, Ng DCH, Jans D, Bogoyevitch M. 2012. Selective STAT3-α or -β expression reveals spliceform-specific phosphorylation kinetics, nuclear retention and distinct gene expression outcomes. Biochem J 447:125–136.

Reich NC. 2009. STAT3 revs up the powerhouse. Sci Signal 2:pe61.

Tammineni P, Anugula C, Mohammed F, Anjaneyulu M, Larner AC, Sepuri NBV. 2013. The import of the transcription factor STAT3 into mitochondria depends on GRIM-19, a component of the electron transport chain. J Biol Chem 288:4723–4732.

Tang QQ, Lane MD. 1999. Activation and centromeric localization of CCAAT/enhancer-binding proteins during the mitotic clonal expansion of adipocyte differentiation. Genes Dev 13:2231–2241.

Tang Q-Q, Otto TC, Lane MD. 2003. Mitotic clonal expansion: A synchronous process required for adipogenesis. Proc Natl Acad Sci USA 100:44–49.

Timofeeva A, Chasovskikh S, Lonskaya I, Tarasova NI, Khavrutskii L, Tarasov SG, Zhang X, Korostyshevskiy VR, Cheema A, Zhang L, Dakshanamurthy S, Brown ML, Dritschilo A. 2012. Mechanisms of unphosphorylated STAT3 transcription factor binding to DNA. J Biol Chem 287:14192–14200.

Tormos KV, Anso E, Hamanaka RB, Eisenbart J, Joseph J, Kalyanaraman B, Chandel NS. 2011. Mitochondrial complex III ROS regulate adipocyte differentiation. Cell Metab 14:537–544.

Wegrzyn J, Potla R, Chwae Y-J, Sepuri NBV, Zhang Q, Koeck T, Derecka M, Szczepanek K, Szelag M, Gornicka A, Moh A, Moghaddas S, Chen Q, Bobbili S, Cichy J, Dulak J, Baker DP, Wolfman A, Stuehr D, Hassan MO, Fu X-Y, Avadhani N, Drake JI, Fawcett P, Lesnefsky EJ, Larner AC. 2009. Function of mitochondrial Stat3 in cellular respiration. Science 323:793–797.

Xu F, Mukhopadhyay S, Sehgal PB. 2007. Live cell imaging of interleukin-6-induced targeting of "transcription factor" STAT3 to sequestering endosomes in the cytoplasm. Am J Physiol Cell Physiol 293:C1374–C1382.

Zhang X, Darnell JE. 2001. Functional importance of Stat3 tetramerization in activation of the alpha 2-macroglobulin gene. J Biol Chem 276:33576–33581.

Zhang Q, Raje V, Yakovlev V, Yacoub A, Szczepanek K, Meier J, Derecka M, Chen Q, Hu Y, Sisler J, Hamed H, Lesnefsky|| EJ, Valerie K, Dent P, Larner AC. 2013. Mitochondrial-localized Stat3 promotes breast cancer growth via phosphorylation of serine 727. J Biol Chem 288:31280–31288.

## SUPPORTING INFORMATION

Additional supporting information may be found in the online version of this article at the publisher's web-site.